NIH-PA Author Manuscript

NIH-PA Author Manuscript

NIH-PA Author Manuscript

Killer Immunoglobulin Receptor 3DL1-mediated recognition of Human Leukocyte Antigen B

Julian P. Vivian[1], **Renee C. Duncan**[1], **Richard Berry**[1], **Geraldine M. O'Connor**[2], **Hugh H. Reid**[1], **Travis Beddoe**[1], **Stephanie Gras**[1], **Philippa M. Saunders**[3], **Maya A. Olshina**[1], **Jacqueline M.L. Widjaja**[3], **Christopher M. Harpur**[3], **Jie Lin**[3], **Sebastien M. Maloveste**[4], **David A. Price**[5,6], **Bernard A.P. Lafont**[4], **Daniel W. McVicar**[2], **Craig S. Clements**[1], **Andrew G. Brooks**[3,#], and **Jamie Rossjohn**[1,5,#]

[1]Department of Biochemistry and Molecular Biology, School of Biomedical Sciences, Monash University, Clayton, Victoria 3800, Australia

[2]Cancer and Inflammation Program, National Cancer Institute-Frederick, Frederick, MD 21702, USA

[3]Department of Microbiology & Immunology, University of Melbourne, Parkville, Victoria 3010, Australia

[4]Non-Human Primate Immunogenetics and Cellular Immunology Unit, Laboratory of Molecular Microbiology, National Institute of Allergy and Infectious Diseases, National Institutes of Health, Bethesda, MD 20892, USA

[5]Department of Infection, Immunity and Biochemistry, Cardiff University School of Medicine, Heath Park, Cardiff CF14 4XN, Wales, UK

[6]Human Immunology Section, Vaccine Research Center, National Institute of Allergy and Infectious Diseases, National Institutes of Health, Bethesda, MD 20892, USA

Abstract

Members of the Killer Immunoglobulin-Like Receptor (KIR) family, a large group of polymorphic receptors expressed on Natural Killer (NK) cells, recognise particular peptide-laden Human Leukocyte Antigen (pHLA) class I molecules and play a pivotal role in innate immune responses[1]. Allelic variation and extensive polymorphism within the three-domain KIR family (KIR3D, domains D0–D1–D2) affects pHLA binding specificity and is linked to the control of viral replication and the treatment outcome of certain haematological malignancies[1–3]. We describe the structure of the KIR3DL1 receptor, bound to HLA-B*5701 complexed with a self-peptide. KIR3DL1 clamped around the C-terminal end of the HLA-B*5701 antigen (Ag)-binding cleft, resulting in two discontinuous footprints on the pHLA. Firstly, the D0 domain, a distinguishing feature of the KIR3D family, extended towards β2-microglobulin and abutted a

region of the HLA molecule that exhibited limited polymorphism, thereby acting as an "innate HLA sensor" domain. Secondly, while the D2-HLA-B*5701 interface exhibited a high degree of complementarity, the D1-pHLA-B*5701 contacts were sub-optimal and accommodated a degree of sequence variation both within the peptide and the polymorphic region of the HLA molecule. While the two-domain KIR (KIR2D) and KIR3DL1 docked similarly onto HLA-C[4,5] and HLA-B respectively, the corresponding D1-mediated interactions differed markedly, thereby providing insight into the specificity of KIR3DL1 for discrete HLA-A and HLA-B allotypes. Collectively, in association with extensive mutagenesis studies at the KIR3DL1-pHLA B*5701 interface, we provide a framework for understanding the intricate interplay between peptide variability, KIR3D and HLA polymorphism in determining the specificity requirements of this essential innate interaction that is conserved across primate species.

HLA-B57 carriage has been associated with delayed progression to AIDS in HIV-infected individuals, with a strong genetic association between the KIR3DL1-HLA-B57 interaction, reduced viral loads and delayed HIV disease progression[3]. We expressed KIR3DL1*001, a prototypical family member, and co-complexed it with HLA-B*5701 bound to a self-peptide (LSSPVTKSF). The affinity (K_D) of this interaction was ≈ 17 μM (Supplementary Table 1, Supplementary Figure 1). We then determined the KIR3DL1*001-HLA-B*5701-LSSPVTKSF structure to 1.8 Å resolution (Supplementary Table 2 & Supplementary Figure 2). KIR3DL1*001 clamped around the C-terminal end of the HLA-B*5701 Ag-binding cleft (Figure 1a–b), forming an extensive interface (total buried surface area (BSA) 1740 Å^2) that encompassed two discontinuous sites – one mediated *via* the D0 domain and the other *via* the D1–D2 domains (Figure 1c–d, 2a–d). KIR3DL1*001 adopted an elongated, zigzag conformation, with the three immunoglobulin (Ig) domains, termed D0, D1 and D2 (residues 7–98, 99–198 and 203–292 respectively) defined by the E-type Ig fold topology (Figure 1a). The D0 domain, a feature of the KIR3D family[6] packed against the D1 domain, the relative juxtapositioning of which (83°) is similar to that of the D1–D2 inter-domain angle (81°), which in turn is analogous to the relative orientation of D1–D2 domains (76°) found in the KIR2D receptors (r.m.s.d. of D1–D2 domains in KIR2DL1 and KIR3DL1 is 1.2 Å) (Supplementary Figure 3a)[4,5]. Further the positioning of the D0 domain relative to the D1 and D2 domains appears to be fixed (Supplementary Figure 3b,c), thereby generating a pre-formed pHLA-binding receptor.

The D0 domain contributed 30% BSA upon complexation with ligand, being orientated almost perpendicular to the main axis of the Ag-binding cleft, extending towards, and just contacting, β2-microglobulin (β2m) (Figure 1a). A surface exposed aromatic cluster (Phe 9, Trp 13, His 29, Phe 34) on one face of the D0 domain ligated to loops 14–18 and 88–92 of HLA-B*5701 (Figure 2a, Supplementary Tables 3 & 4), both of which flexed slightly upon KIR3DL1*001 binding (Supplementary Figure 4)[7]. These two HLA loops exhibit very limited polymorphism amongst the HLA-A and HLA-B alleles and mostly have main chain interactions with the D0 domain, thereby indicating that the D0-HLA interactions are largely independent of sequence variation and likely to be conserved across most HLA alleles. Lengthening or shortening the HLA-B*5701 loop (residues 14–18) markedly reduced binding to KIR3DL1*001 (Figure 3a). Alanine substitution of Ser 11, His 29 and particularly Phe 9 in KIR3DL1*001 impaired binding of HLA-B*5701 tetramers, further highlighting the importance of the D0 contacts (Figure 3b). Interestingly, the site of the D0-mediated interaction on HLA-B*5701 has not, to the best of our knowledge, been observed in any HLA-binding immune receptor/coreceptor to date, indicating a unique molecular recognition signature, in which the D0 domain acts as an "innate sensor" of an essentially invariant region of HLA molecule.

The D1–D2 domains converged to form a continuous binding interface with HLA-B*5701 (Figure 1c–d), interacting with residues from the α1- and α2-helices flanking the P8 position of the peptide. The ligand-binding site of the D1–D2 domains was relatively flat, facilitating the close positioning of HLA B*5701, resulting in an intricate network of interactions across the interface; as such, the total BSA upon complexation at the D1–D2 interaction site was quite large (total BSA 1360 Å^2). The D1 and D2 domains contributed 600 and 760 Å^2 total BSA to the interface respectively, with the D1 domain docked above the α1-helix and contacting the peptide, whereas the D2 domain sat above the α2-helix, thereby providing immediate insight into the disparate roles that the D1 and D2 domains play in HLA-B*5701 engagement (Figure 1c–d). The D2 domain predominantly interacted with a region spanning residues 142–151 of HLA-B*5701 (Supplementary Table 3), a region that displays limited polymorphism amongst HLA-B alleles. At the core of the D2-HLA-B*5701 binding interface, two aromatic residues of KIR3DL1*001, Tyr 200 and Phe 276, converged onto the α2-helix, while polar interactions were located at the periphery (Figure 2b). A feature of this interface was the centrally located Glu 282 of KIR3DL1*001, a charged residue that abuts Leu 166 from the D1 domain, yet is stabilized by polar interactions with Tyr 200 and Ser 279 of KIR3DL1*001, Lys146 of HLA-B*5701 and water-mediated interactions with the peptide and Arg 83 on the α1-helix (Figure 2c). Alanine substitution of Glu 201, Ser 227, Asp 230 or His 278, residues that were located at the exterior of the interface, had little impact on binding (Figure 3b). In contrast, alanine substitution of Tyr 200 or Phe 276, which formed the central aromatic cluster, or the charged residue, Glu 282, abrogated tetramer binding (Figure 3b). Further, of the five HLA-B*5701 mutations made at the D2-HLA-B*5701 interface, three residues (Ile 142, Lys 146 and Ala 149) markedly impacted on the affinity of the interaction (Figure 3a). These three HLA B*5701 residues interacted principally with the Tyr 200 and Phe 276, further highlighting the importance of this internal core of KIR3DL1*001 residues in driving the D2-HLA-B*5701 interaction. Collectively, the D2-HLA-B*5701 binding site appears to have co-evolved to form a highly complementary binding interface.

KIR3DL1 recognises HLA class I allotypes that contain the Bw4 serological epitope spanning residues 77–83 on the α1-helix[8,9]. While the D1 domain was positioned over the Bw4 epitope making contacts with residues 79, 80 and 83, it interacted with a broader region of the α1-helix, including Gln 72, which bound to Met 165 (Figure 2d, Supplementary Table 3). In marked contrast to the D2-mediated contacts, the D1-HLA-B*5701 interface appeared to largely lack both charge and shape complementarity (Figure 2d, Supplementary Figure 5). Among the residues within the Bw4 motif, Arg 79 formed van der Waals (vdw) contacts with Ser 140 and H-bonded to the main chain of Gly 138. Nevertheless the environment of Arg 79 was sub-optimal, with its sidechain being in close proximity to Lys 136 and Ile 139 of KIR3DL1*001. Ile 80, a residue previously associated with KIR3DL1 reactivity[10] formed a single vdw contact with Leu 166 and was positioned within a small hydrophobic cavity created by Glu 76, Arg 79 and Arg 83, a triad of HLA-B*5701 residues that leaned towards each other to form an array of salt-bridging interactions (Figure 2d). Further, Arg83 from the Bw4 motif packed against and H-bonded to the main chain of His 278 (Figure 2d). Surprisingly none of the five alanine mutations introduced into the D1 domain significantly impacted on the KIR3DL1-pHLA-B*5701 interaction (Figure 3b). However, in contrast, mutation of the corresponding HLA-B*5701 contact residues did impact on recognition, particularly the Ile80Ala and Arg83Ala mutations (Figure 3a). Interestingly, mutation of Ile 80 to Thr, a natural dimorphism within the Bw4 motif, reduced the affinity of the interaction with KIR3DL1*001 modestly (Figure 3a). Presumably, the Ile80Ala and Ile80Thr mutations differentially disrupt the conformation of the Glu 76-Arg 79-Arg 83 triad, thereby affecting KIR3DL1 recognition. Thus while KIR3DL1*001 contacted the highly polymorphic region of the HLA class I in a non-optimal manner, and the D1 residues were shown to be non-essential for this interaction, modifications within the HLA itself impacted on the D1-HLA-

B*5701 interaction and thus could serve to fine-tune the specificity of the interaction. Indeed, while KIR3DL1*001 specifically binds HLA alleles that possess the Bw4 motif, it does not interact with the closely related Bw6 motif, which possesses a Gly at position 83. Accordingly our data provides a basis for understanding the significance of polymorphism at residue 83 for KIR3DL1 recognition of the Bw4+ epitope[2].

The D1 domain interacted with the LSSPVTKSF peptide, however the sole direct interaction between the peptide and KIR3DL1*001 was a vdw contact between P8-Ser[OG] and Leu 166 (Figure 2c). Thus, KIR3DL1*001 made limited contact with the peptide, analogous to the interactions observed between KIR2D and peptides bound to HLA-C[4,5], and in marked contrast to CD94-NKG2A recognition of HLA-E[11]. To probe the role of peptide in the interaction, a series of peptides that were substituted at P8 were refolded with HLA-B*5701 and assessed for their impact on recognition by KIR3DL1*001. The Phe, His and Arg P8 substitutions all facilitated an interaction with KIR3DL1*001, albeit with lower affinities, suggesting that the receptor interface has capacity to tolerate large side-chains at P8, consistent with the presence of a solvent filled cavity adjacent to the P8 position at the KIR3DL1-pHLA-B*5701 interface. In contrast, the Ala, Glu and Leu P8 substitutions markedly reduced the corresponding interaction affinities (Supplementary Table 1, Supplementary Figure 1), suggesting that the KIR3DL1*001 receptor can "discriminate" between peptides. The basis for the differential effects of the P8 residue could be attributable either to direct steric hindrance/lack of complementarity between the peptide and KIR3DL1*001, or to conformational alteration of the residues within the Bw4 motif itself[12]. Collectively, our observations are consistent with previous studies[13,14], which demonstrated that the sequence of the bound peptide could have a profound impact on HLA recognition by KIR.

Next, we assessed the underlying HLA specificities of the KIR2DL and KIR3DL receptor families[4,5] (Supplementary Figures 6 & 7). The D1–D2 domains of KIR3DL1*001 share clear sequence and structural homology with the HLA-C-reactive receptors, KIR2DL1, -2 and -3[4,5,15] and there are a number of similarities in the recognition of the α2-helix by both KIR2DL1 and -2 and KIR3DL1*001 (Supplementary Figure 7). In contrast, the interactions between the KIR3DL1 and KIR2DL1 receptors and the α1-helices of their respective HLA class I ligands differ (Supplementary Figure 6b). These differences principally arise from the loop regions that connect the C and C′ β-strands and the E and F strands in the D1 domain and the F and F′ β-strands that bridge the D1 and D2 domains. For example, the CC′ loop in the KIR2DL receptors adopts a notably different conformation from that observed in KIR3DL1 (Supplementary Figure 6c). In KIR3DL1, this loop (137–140) is mostly flat and featureless, sitting adjacent to the α1-helical axis, forming limited contacts with HLA-B*5701. In the KIR2DL receptors, the corresponding loop region (42–45) is orientated towards the α1-helix, and contains two prominent residues that would prevent binding to HLA B*5701 due to steric hindrance with residues within the Bw4 motif. Thus, the D1-mediated contacts are critical for the HLA specificity differences between the KIR2DL and KIR3DL1 families.

The KIR3D family comprises the KIR3DL1/S1, KIR3DL2 and KIR3DL3 proteins[16]. More than 200 alleles within the KIR3D family have been described, with KIR3D allomorphs generally differing from each other by a limited number of amino acids[17]. Given the high sequence identity between KIR3DL1*001 and KIR3DL2, KIR3DL3 and KIR3DS1 receptors (86, 74, 97% respectively), the KIR3DL1*001-HLA-B*5701 structure provided a template to examine the impact of sequence variation across the entire KIR3D family and relate this to pHLA specificity.

Sequence and structural analyses suggested that a "hot-spot" resided within the D1–D2 domains, comprising loops 165–167, 199–201 and 278–282, all of which converged to form an intricate bonded network that centered on Glu 282 (Figure 4a–e). Variation within these three loops could potentially alter the conformation of neighbouring residues within this "hot-spot" region, thereby impacting on receptor specificity. KIR3DS1 is distinct amongst the KIR3D family in that it is an activating receptor. Genetic data have shown that KIR3DL1 and KIR3DS1 are allelic variants of the same gene and suggested that KIR3DS1 interacts with HLA-Bw4 molecules bearing an Ile at residue 80 (Bw4+I80)[18]. However direct evidence of an interaction between KIR3DS1 and Bw4+I80 molecules is lacking[19]. Four positions that differ between KIR3DL1 and KIR3DS1 map to the KIR3DL1*001-pHLA-B*5701 interface and thus may impact on the interaction (Figure 4c), consistent with recent observations using HLA-A24 tetramers[20,21]. While the Gly138Trp and Pro199Leu mutations had little impact on HLA-B*5701 binding, mutation of Leu166 which is located within the hotspot to Arg significantly diminished tetramer binding (Figure 4f), thereby providing a basis why KIR3DS1 cannot bind HLA-B*5701.

The KIR3DL2 family recognizes a limited subset of HLA-A alleles[22,23], with seven sequence differences that map to the "hot-spot" region (Figure 4d). The introduction of these residues into KIR3DL1*001 showed that while the Leu166Pro, Ala167Val (Figure 4f) and His278Ala mutations (Figure 3b) did not impair recognition of HLA-B*5701, the Ser279Leu and Glu282Val mutations markedly reduced tetramer binding (Figure 4f). Removal of the charged moiety of Glu282 would disrupt the intricate network of interactions at the KIR3DL1-pHLA-B5701 interface. While the Ser279Ala mutation did not abrogate HLA-B*5701 binding (Figure 3b), the impact of the Ser279Leu mutation was much more pronounced. This effect appears attributable to the more bulky Leu residue causing a steric clash with Arg83, thereby suggesting a basis for the lack of reactivity of KIR3DL2 towards the Bw4 motif. Moreover unlike HLA-B*5701 and other HLA-Bw4 allotypes, HLA-A3 and HLA-A11 possess a Gly at position 83 rather than Arg, which is a crucial determinant for KIR3DL1 recognition of the Bw4 motif[2].

The specificity of the KIR3DL3 receptor family is undefined, and a number of differences between KIR3DL1 and –3DL3 reside within the "hot-spot" region (Figure 4e). Binding experiments showed that the Met165Thr or Leu166Pro substitutions in KIR3DL1*001 did not impact on HLA-B*5701 binding (Figure 4f). Further, while the Pro199Leu substitution had a modest impact on recognition, the Glu282Ala substitution within KIR3DL1 totally abrogated tetramer binding (Figure 3b), thereby indicating that residues 279 and 282 are critical determinants of the specificity differences between KIR3DL1 and other KIR3D family members.

Surprisingly, the extensive polymorphism amongst the inhibitory receptors within each KIR3D family was predominantly located at sites not directly implicated in pHLA binding (Figure 4b). Collectively, these observations suggest that the majority of KIR3D polymorphisms within a family[24,25] are unlikely to directly affect the affinity of the pHLA interaction *per se*, but rather are likely to impact on pHLA binding via altering expression levels and/or the clustering of the KIR3D receptors on the cell surface, whereas sequence differences across the KIR3D family directly impact on pHLA affinity and specificity. Indeed, functional studies have shown that polymorphisms in residues such as 238 that are distant from the receptor/ligand interface can impact on target cell recognition by KIR3DL1^{+} NK cells[26].

Collectively our data provide a fundamental basis for understanding how a representative KIR3DL family member interacts with an HLA-B allele that possesses the Bw4 motif. We show that the D0 domain, a feature of this family, interacts with a previously unrecognized

determinant on the HLA molecule, which is highly conserved across HLA-A and HLA-B alleles in particular. These observations suggest that the D0 domain acts as an "innate HLA sensor" at a site that that is not involved in either peptide or TCR binding[27]. The KIR3DL interaction sites appear to be largely conserved across the KIR3D family, with specificity differences mapping to a "hot-spot" within the interaction interface. In contrast, the polymorphisms within individual KIR3D gene families are largely at positions that are spatially separate from the binding site, a number of which are the subject of positive selection[17]. This suggests that other evolutionary pressures, such as pathogen-mediated immune evasion strategies may drive KIR3D diversification at sites distant from the ligand-binding site.

Methods

Protein expression and purification

HLA B*5701 and β_2-microglobulin ($\beta 2m$) were expressed separately in *E. coli* from the pET-30 vector. Inclusion body preparations of the HLA B*5701 and β_2m were refolded and purified as detailed previously[7]. In brief, the resultant HLA class I complexes were purified by DEAE sepharose (Sigma) anion exchange chromatography using 10 mM Tris pH 8.0 and eluted with 150 mM NaCl. The protein was then further purified by gel filtration using an S200 16/60 column (GE Healthcare). The final purification step utilised anion exchange chromatography on a MonoQ column (GE Healthcare). The binary complex was concentrated in 10 mM Tris pH 8.0, 150 mM NaCl for use in crystallisation trials and SPR studies. The mutants of HLA-B*5701 were generated using the QuikChange PCR method (Stratagene) and purified as above.

Residues 1 to 299 of KIR3DL1*001 were cloned into the pHLSec mammalian expression vector with N-terminal 6xHis and secretion tags. KIR3DL1 was expressed from transiently transfected HEK 293S cells. Secreted KIR3DL1 was harvested from the culture media three days after transfection by firstly dialysing the media against 10 mM Tris pH 8.0, 300 mM NaCl prior to the use of nickel affinity resin. The KIR3DL1 was eluted from the nickel resin with 10 mM Tris pH 8.0, 300 mM NaCl, 50 mM EDTA. The protein was purified by gel filtration chromatography using an S200 16/60 column (GE Healthcare) in 10 mM Tris pH 8.0, 300 mM NaCl. Purified KIR3DL1 was then concentrated to 15 mg/ml and deglycosylated with endoglycosidase H (New England Biolabs.). The extent of deglycosylation was monitored by SDS-PAGE and this material was used in crystallisation trials. For SPR studies a similar construct of KIR3DL1*001 was prepared in the pFastBac vector and expressed from Hi-5 insect cells (Invitrogen). The KIR3DL1*001 was purified as above with the exception that the endoglycosidase H deglycosylation step was not performed.

Crystallisation and data collection

The KIR3DL1*001-pHLA-B*5701 complex at 15 mg/ml was crystallised at 294 K by the hanging-drop vapour-diffusion method from a solution comprising 16 % PEG 3350, 2 % tacsimate pH 5 and 0.1 M tri-sodium citrate pH 5.6. The crystals typically grew to dimensions $0.3 \times 0.3 \times 0.2$ mm in 7 days. Prior to data collection, the crystals were equilibrated in crystallisation solution with 35 % PEG 3350 added as a cryoprotectant and then flash-cooled in a stream of liquid nitrogen at 100 K. X-ray diffraction data were recorded on a Quantum-315 CCD detector at the MX2 beamline of the Australian Synchrotron. The data were integrated and scaled using DENZO and SCALEPACK from the HKL2000 program suite. Details of the data processing statistics are given in Supplementary Table 2. The final model comprises residues 6–261, 267–292 and there are three glycosylation site located at Asn 71, Asn 158 and Asn 252.

Structure determination and refinement

The structure was determined by molecular replacement using MOLREP. The search models used were the structures of HLA-B*5701 and KIR2DL1 (PDB codes 2RFX and 1IM9). The positions of the two complexes in the asymmetric unit were found in an incremental manner. The orientation of the first HLA molecule was found and subsequently the position of the D1 and D2 domains of the KIR receptor were placed. The second complex was fitted by application of the pseudo-translation vector 0.0, 0.5, 0.5.

Refinement of the model was carried out in REFMAC with strict two-fold NCS applied. Structure building proceeded with iterative rounds of manual building in COOT and refinement in REFMAC. The D0 domain of KIR3DL1 was manually built from the resultant electron density maps. The NCS restraints were removed for the final rounds of refinement. Solvent was added with COOT and the structure validated with MOLPROBITY[29]. The final structure comprises two KIR3DL1-pHLA-B*5701 complexes in the asymmetric unit, the association of which did not suggest higher order oligomeric assemblies within the crystal lattice. The final refinement values are summarized in Supplementary Table 2. The crystals contained two virtually indistinguishable ternary complexes within the asymmetric unit, so structural analyses were confined to one KIR3DL1*001-pHLA-B*5701 complex.

Transfection studies

The sequence for a FLAG tag (GACTACAAAGACGATGACGACAAG) was added to the 5' end of KIR3DL1*001 by primer addition and this cDNA was then cloned into a pEF6 vector. Specific nucleotide residues were mutated using the QuikChange II Site Directed Mutagenesis Kit (Stratagene) according to the manufacturer's instructions using PAGE-purified primers. The sequence was verified by direct sequencing. These constructs were introduced into HEK293T cells using FuGene® 6 transfection reagent (Roche) according to the manufacturer's instructions. After 48 hours, the cells were harvested and stained with anti-FLAG (clone M2, Sigma Aldrich) antibody or with tetramer for 30 minutes at 4°C. The cells were then washed and analysed on a Fortessa flow cytometer (BD Biosciences). Analysis of cell surface expression as assessed by staining with anti-FLAG mAb showed that the introduction of the mutations had no substantial effect on expression (data not shown). All transfection data are representative of two independent experiments.

Surface plasmon resonance

SPR experiments were conducted at 25°C on a Biacore 3000 instrument using HBS buffer (10 mM HEPES-HCl (pH 7.4), 150 mM NaCl, and 0.005% surfactant P20 supplied by the manufacturer). The HLA class I-specific antibody W6/32 was immobilized on a CM5 chip via amine coupling according to manufacturer's instructions. The pHLA complexes, and mutants thereof, were captured by W6/32 creating a surface density of approximately 500–1000 RU. Various concentrations of KIR3DL1*001 (2.37 to 300μM) were injected over the captured pHLA at 5 μl/min. The final response was calculated by subtracting the response of W6/32 alone from the KIR3DL1*001-pHLA-B*5701 complex. The equilibrium data were analyzed using GraphPad Prism. The shortened form of HLA-B*5701 comprised Gly-Gly-Gly in place of residues 14–19; in the long form of HLA-B*5701, Gly-Gly-Gly was inserted after Gly 16. For the SPR experiments, data are representative of two independent experiments with error bars representing S.E.M. of the duplicates.

Supplementary Material

Refer to Web version on PubMed Central for supplementary material.

Acknowledgments

References

1. Parham P. MHC class I molecules and KIRs in human history, health and survival. Nat Rev Immunol. 2005; 5:201–214. [PubMed: 15719024]

2. Sanjanwala B, Draghi M, Norman PJ, Guethlein LA, Parham P. Polymorphic Sites Away from the Bw4 Epitope That Affect Interaction of Bw4+ HLA-B with KIR3DL1. The Journal of Immunology. 2008; 181:6293–6300. [PubMed: 18941220]

3. Martin MP, et al. Innate partnership of HLA-B and KIR3DL1 subtypes against HIV-1. Nat Genet. 2007; 39:733–740. [PubMed: 17496894]

4. Boyington JC, Motyka SA, Schuck P, Brooks AG, Sun PD. Crystal structure of an NK cell immunoglobulin-like receptor in complex with its class I MHC ligand. Nature. 2000; 405:537–543. [PubMed: 10850706]

5. Fan QR, Long EO, Wiley DC. Crystal structure of the human natural killer cell inhibitory receptor KIR2DL1-HLA-Cw4 complex. Nat Immunol. 2001; 2:452–460. [PubMed: 11323700]

6. Colonna M, Samaridis J. Cloning of immunoglobulin-superfamily members associated with HLA-C and HLA-B recognition by human natural killer cells. Science. 1995; 268:405–408. [PubMed: 7716543]

7. Chessman D, et al. Human leukocyte antigen class I-restricted activation of CD8+ T cells provides the immunogenetic basis of a systemic drug hypersensitivity. Immunity. 2008; 28:822–832. [PubMed: 18549801]

8. Litwin V, Gumperz J, Parham P, Phillips JH, Lanier LL. NKB1: a natural killer cell receptor involved in the recognition of polymorphic HLA-B molecules. J Exp Med. 1994; 180:537–543. [PubMed: 8046332]

9. Gumperz JE, Litwin V, Phillips JH, Lanier LL, Parham P. The Bw4 public epitope of HLA-B molecules confers reactivity with natural killer cell clones that express NKB1, a putative HLA receptor. J Exp Med. 1995; 181:1133–1144. [PubMed: 7532677]

10. Cella M, Longo A, Ferrara GB, Strominger JL, Colonna M. NK3-specific natural killer cells are selectively inhibited by Bw4-positive HLA alleles with isoleucine 80. J Exp Med. 1994; 180:1235–1242. [PubMed: 7931060]

11. Petrie EJ, et al. CD94-NKG2A recognition of human leukocyte antigen (HLA)-E bound to an HLA class I leader sequence. The Journal of Experimental Medicine. 2008; 205:725–735. [PubMed: 18332182]

12. Hulsmeyer M, et al. Thermodynamic and Structural Equivalence of Two HLA-B27 Subtypes Complexed with a Self-peptide. Journal of Molecular Biology. 2005; 346:1367–1379. [PubMed: 15713487]

13. Peruzzi M, Parker KC, Long EO, Malnati MS. Peptide sequence requirements for the recognition of HLA-B*2705 by specific natural killer cells. J Immunol. 1996; 157:3350–3356. [PubMed: 8871631]

14. Fadda L, et al. Peptide antagonism as a mechanism for NK cell activation. Proceedings of the National Academy of Sciences. 2010; 107:10160–10165.

15. Maenaka K, et al. Killer Cell Immunoglobulin Receptors and T Cell Receptors Bind Peptide-Major Histocompatibility Complex Class I with Distinct Thermodynamic and Kinetic Properties. J. Biol. Chem. 1999; 274:28329–28334. [PubMed: 10497191]

16. Trowsdale J, et al. The genomic context of natural killer receptor extended gene families. Immunol Rev. 2001; 181:20–38. [PubMed: 11513141]

17. Norman PJ, et al. Unusual selection on the KIR3DL1/S1 natural killer cell receptor in Africans. Nat Genet. 2007; 39:1092–1099. [PubMed: 17694054]

18. Martin MP, et al. Epistatic interaction between KIR3DS1 and HLA-B delays the progression to AIDS. Nat Genet. 2002; 31:429–434. [PubMed: 12134147]

19. Carr WH, et al. Cutting Edge: KIR3DS1, a Gene Implicated in Resistance to Progression to AIDS, Encodes a DAP12-Associated Receptor Expressed on NK Cells That Triggers NK Cell Activation. The Journal of Immunology. 2007; 178:647–651. [PubMed: 17202323]

20. Sharma D, et al. Dimorphic motifs in D0 and D1+D2 domains of killer cell Ig-like receptor 3DL1 combine to form receptors with high, moderate, and no avidity for the complex of a peptide derived from HIV and HLA-A*2402. J Immunol. 2009; 183:4569–4582. [PubMed: 19752231]

21. O'Connor GM, et al. Analysis of Binding of KIR3DS1*014 to HLA Suggests Distinct Evolutionary History of KIR3DS1. The Journal of Immunology. 2011

22. Dohring C, Scheidegger D, Samaridis J, Cella M, Colonna M. A human killer inhibitory receptor specific for HLA-A1,2. J Immunol. 1996; 156:3098–3101. [PubMed: 8617928]

23. Hansasuta P, et al. Recognition of HLA-A3 and HLA-A11 by KIR3DL2 is peptide-specific. Eur J Immunol. 2004; 34:1673–1679. [PubMed: 15162437]

24. Yawata M, et al. Roles for HLA and KIR polymorphisms in natural killer cell repertoire selection and modulation of effector function. The Journal of Experimental Medicine. 2006; 203:633–645. [PubMed: 16533882]

25. Khakoo SI, Geller R, Shin S, Jenkins JA, Parham P. The D0 domain of KIR3D acts as a major histocompatibility complex class I binding enhancer. J Exp Med. 2002; 196:911–921. [PubMed: 12370253]

26. Carr WH, Pando MJ, Parham P. KIR3DL1 polymorphisms that affect NK cell inhibition by HLA-Bw4 ligand. J Immunol. 2005; 175:5222–5229. [PubMed: 16210627]

27. Godfrey DI, Rossjohn J, McCluskey J. The Fidelity, Occasional Promiscuity, and Versatility of T Cell Receptor Recognition. Immunity. 2008; 28:304–314. [PubMed: 18342005]

28. Aricescu AR, Lu W, Jones EY. A time- and cost-efficient system for high-level protein production in mammalian cells. Acta Crystallographica Section D. 2006; 62:1243–1250.

References

29. Davis IW, et al. MolProbity: all-atom contacts and structure validation for proteins and nucleic acids. Nucleic Acids Research. 2007; 35:W375–W383. [PubMed: 17452350]
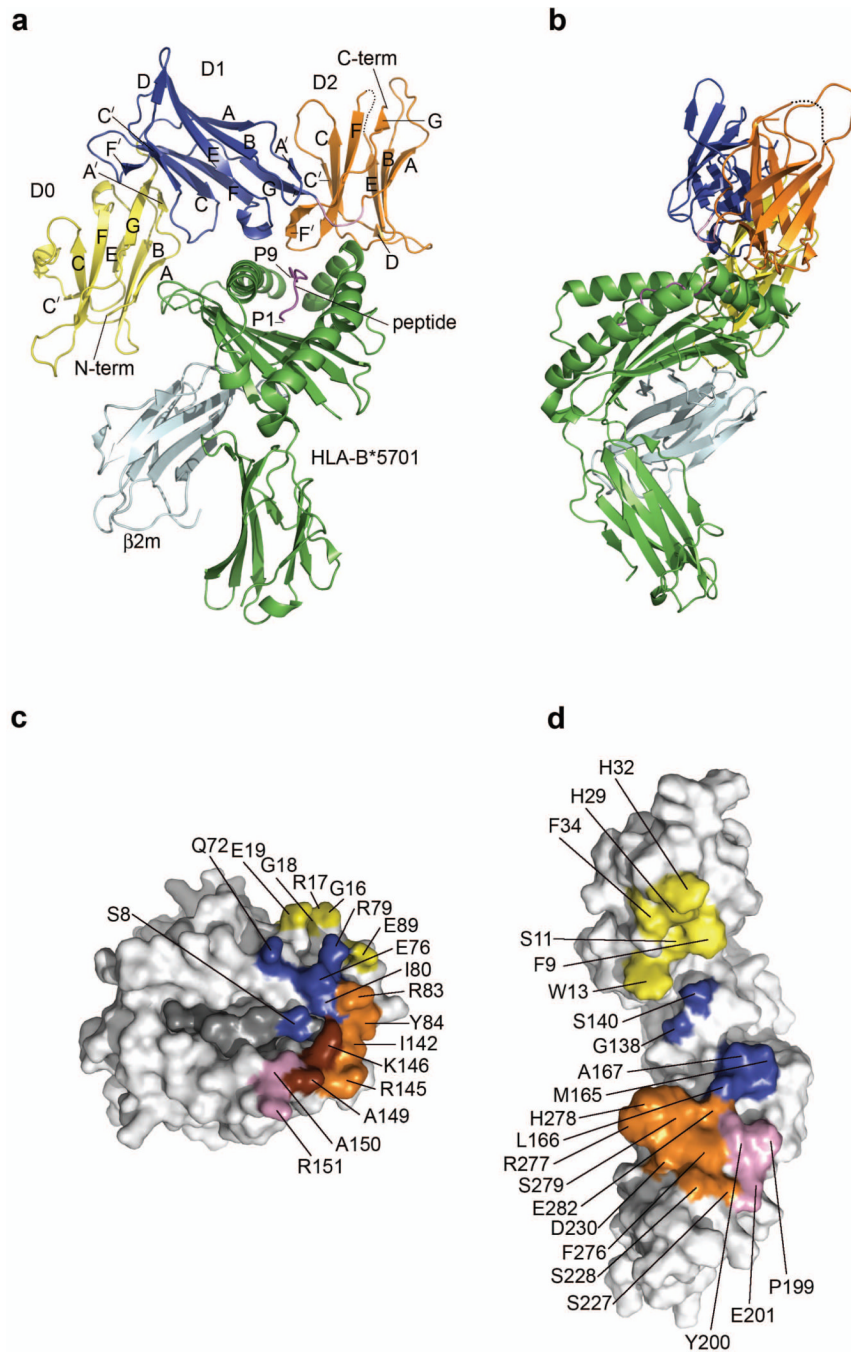
Figure1. Structure of the KIR3DL1*001 HLA-B*5701 complex
(*a*) and (*b*) Orthogonal views of the complex with the KIR3DL1 strands labeled. The HLA and β2m are coloured green and cyan, respectively; D0, D1, D1–D2 loop, and D2 are coloured yellow, blue, pink and orange respectively; dashed line represents the unresolved loop between the E and F strands. (*c*) and (*d*) The footprint mapped to the surface of HLA and KIR3DL1, respectively, with residues coloured in each case according to the interacting KIR3DL1 domain: D0 (yellow), D1 (blue), D1–D2 loop (pink), and D2 (orange). Residues that contact the linker and the D2 domain are coloured brown.
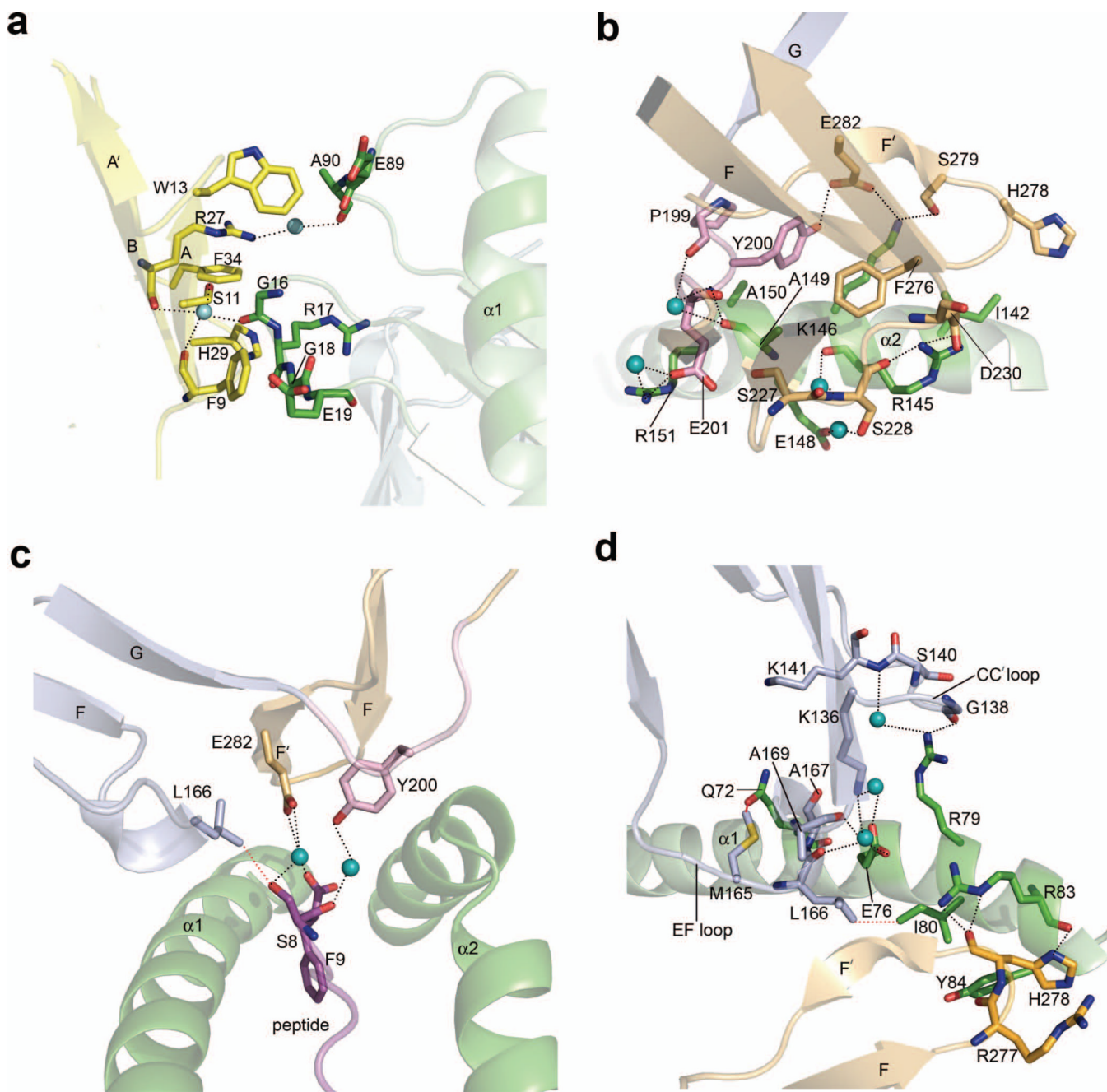
Figure 2. Contacts between the KIR3DL1*001 receptor and the pHLA-B*5701
Contacts between (*a*) the D0 domain and the HLA, (*b*) KIR3DL1*001 and the HLA α2-helix, (*c*) KIR3DL1*001 and the peptide, and (*d*) KIR3DL1*001 and the HLA α1-helix. The VDW contacts between Leu 166 and P8-Ser, Leu166 and Ile80, and Met165 and Gln72, are shown as red dashed lines. (b) Tyr200 packed against Ala149, Ala150 and Lys146, while Phe276 nestled between Arg145 and Lys146, and contacted Ala149. At the periphery, Arg145 and Arg151 from HLA-B*5701 salt-bridged to Asp230 and Glu201, respectively. Coloured as in Figure 1; water molecules, cyan spheres; hydrogen bonds, dashed lines.
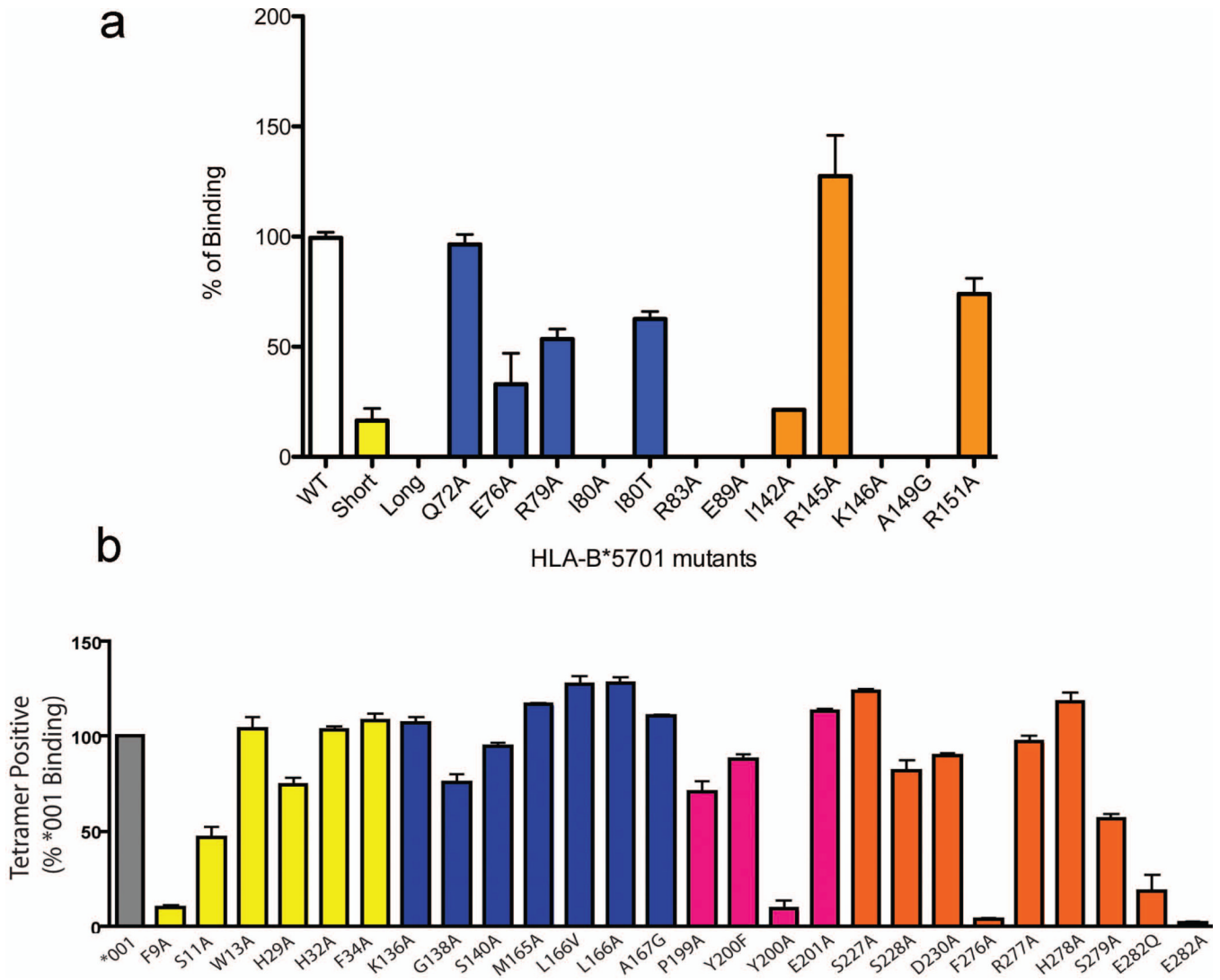
Figure 3. Mutational analysis at the KIR3DL1*001-pHLA-B*5701 interface
(*a*) SPR-based affinity measurements of the KIR3DL1*001 interaction with HLA-B*5701 mutants. Results are expressed as a % of the wild-type interaction; mutants are colour-coded according to the KIR3DL1*001 domain they contact to correspond with Figure 1. (*b*) Capacity of HLA-B*5701 tetramers to bind 293T cells transfected with plasmids encoding either a FLAG-tagged KIR3DL1 or 26 single site-directed mutants. HLA-B*5701 tetramers, but not HLA-B*0801 tetramers (data not shown), bound 293T cells transfected with KIR3DL1*001. Binding is expressed as a proportion of positive cells relative to cells transfected with wild-type KIR3DL1*001. Mutated residues are colour-coded as in Figure 1. N=2 independent experiments; error bars represent S.E.M.
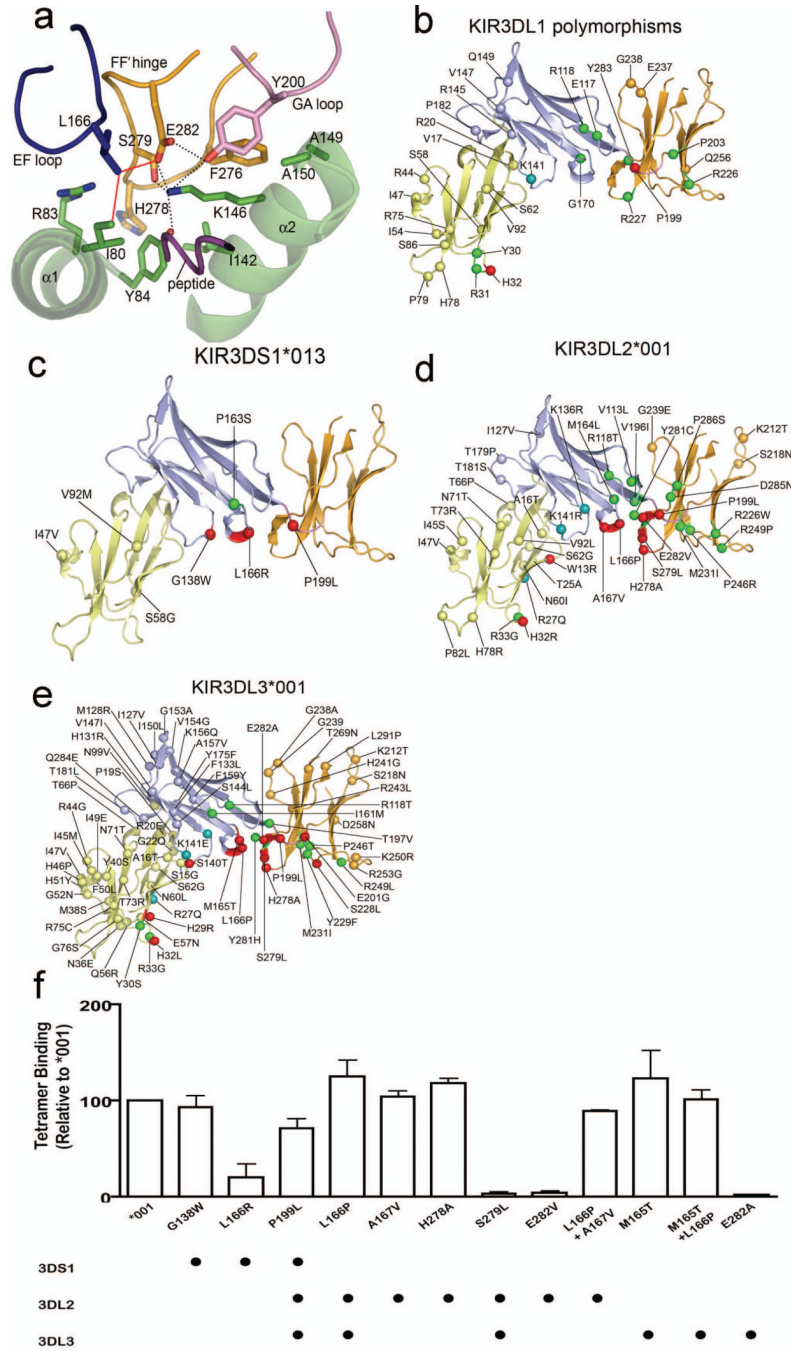
Figure 4. Mapping of polymorphisms and sequence variations onto the structure of KIR3DL1*001

(a) The "hot-spot" is represented by three loops. *(b)* Polymorphisms within the KIR3DL1 family. *(c–e)* Differences between KIR3DS1*013 and KIR3DL1*001 *(c)*, KIR3DL2*001 and KIR3DL1*001 *(d)*, KIR3DL3*001 and KIR3DL1*001 *(e)*. Polymorphisms are represented as spheres: red, direct contacts in the KIR3DL1*001-pHLA-B*5701 structure; cyan, water-mediated contacts; green, residues that may affect binding; other, remaining residues coloured according to domain. *(f)* The capacity of HLA-B*5701 tetramers to bind to 293T cells transfected with plasmids encoding either a FLAG-tagged KIR3DL1*001 or 10 site-directed mutants representing sites of 3DL1/2/3 or 3DS1 variation that were

contacted by HLA-B*5701. N=2 independent experiments; error bars represent S.E.M. Variations across the KIR3D family are shown underneath.